ETH Zurich

Semester Thesis

Characterization of superconducting resonators

Raoul W. Scherwitzl
Major: Physics MSc
Supervisor: Univ.-Prof. Dr. Andreas Wallraff,
Laboratorium für Festkörperphysik, ETH Zürich

Zurich, 18/12/2007

Contents

1 Introduction

Quantum computers were first proposed in the 1970s and 1980s by theorists such as R. Feynman, Paul Benioff, David Deutsch and Charles Benett. The usefulness of their implementation was often doubted until the mid-nineties when Peter Shor discovered a quantum algorithm for factorizing large numbers exponentially faster than conventional computers. Tremendous progress has been made since then in the realm of applied quantum mechanics.

Integrated circuit components of classical computers are approaching the so-called "quantum limit". It is therefore an appealing idea to exploit quantum effects for better computation instead of avoiding them. A large scale quantum computer could have a huge impact in the area of encryption and decryption, as well as powerful equipment for solving highly complex computational problems in all sorts of research fields (e.g. biology, chemistry, mathematics), it could also provide faster search engines, and help us simulate quantum systems.

In a conventional computer, information is stored as an electrical charge, representing a bit, being either in the state 0 or 1. A quantum computer is realized with qubits which can be in the states $|0\rangle$,$|1\rangle$, or in a superposition of these states. Possible candidates for qubits are ion traps, nuclear and electron spins, neutral atoms, photons and superconducting circuits.

Superconducting circuits are a very promising approach since they can be easily implemented in an electrical circuit. The nonlinearity of Josephson junctions can be used to construct two-level quantum systems (qubits). The idea consists of coupling a superconducting qubit to a superconducting waveguide resonator. The resonator would act as a cavity by isolating the incoming photons and making measurements of quantum processes possible. It is therefore important to fabricate high quality factor resonators. The resonators need to be characterized and studied thoroughly before proceeding with the fabrication of the qubit itself.

This semester work divides up into two major parts which are the fabrication of microwave frequency superconducting resonators and their characterization by measurements at low temperatures. Superconducting materials that have been used were Niobium with $T_c = 9.2\,^{\circ}\mathrm{K}$ allowing measurements in liquid helium at $4.2\,^{\circ}\mathrm{K}$ as well and Aluminum with $T_c = 1.2\,^{\circ}\mathrm{K}$ requiring measurements in a low temperature cryostat.

2 Theoretical background

An electromagnetic field can be described by a collection of photons occupying different modes (k, λ) with their occupation number $N(k, \lambda)$ where k is the wavevector and λ its polarization The energy of the field is given by

$$\begin{aligned} E &= \sum_{k,\lambda} \hbar |k| \, cN(k, \lambda) \\ &= \sum_{k,\omega} \hbar\omega N(k, \omega) \qquad \text{with } \omega = |k| \, c \end{aligned} \tag{1}$$

For an integrated circuit to behave quantum mechanically, the two requirements are

1. low dissipation
2. low noise

In the first case, all metallic parts need to have zero resistivity, more precisely, they need to be superconducting. In the second case, the thermal fluctuation with energy kT should be sufficiently lower than the transition energy $\hbar\omega$ between the ground state $|0\rangle$ and the first excited state $|1\rangle$. The frequency for superconducting circuits is typically between 2 GHz and 20 GHz . If we work at higher temperatures, e.g. in liquid helium, more noise is expected.

To enter the cavity-QED regime one needs a cavity which will couple to the qubit. In this work a coplanar waveguide resonator has been used. The higher modes of the resonator should not be close to qubit's transition frequency. The external capacitances confine the photons, reflect them back and forth and increases the chances to interact with the atom.

2.1 Mapping of transmission line resonance to LC resonance

Around its resonance frequency a transmission line resonator behaves like a parallel LCR circuit, where L, C and R can be expressed in terms of quantities per unit length of a transmission line. Below, I give a short overview over the theory of resonators which is discussed extensively in [1], [2] and [3].

2.1.1 Parallel LC Resonator

The circuit as shown in Fig. 1 is described by its impedance $Z(\omega)$ which, in the case of a parallel LCR oscillator, is given by

$$Z_{\mathrm{LCR}}(\omega) = \left[\frac{1}{R} + \frac{1}{i\omega L} + i\omega C \right]^{-1} \tag{2}$$

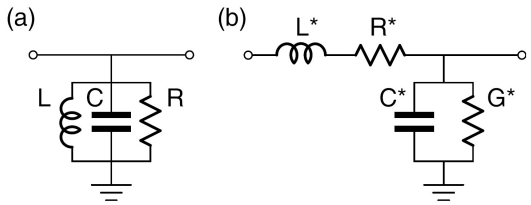

Figure 1: *a) Parallel LCR resonator. b) Transmission line model. Figure taken from [3].*

with R being the resistance, L the inductance and ω the frequency. The impedance can be approximated by, see e.g. [1]

$$Z_{\mathrm{LCR}}(\omega) \approx \frac{R}{1 + 2iQ\frac{\omega-\omega_0}{\omega_0}} \tag{3}$$

where $Q = \omega_0 RC$ is the quality factor of the resonator.

The temporal response of the parallel LCR resonator can be written as

$$\ddot{I} + \frac{1}{RC}\dot{I} + \frac{1}{LC}I = 0 \tag{4}$$

with the solution

$$I(t) = I_L 0 e^{[i\omega_0 t - \frac{1}{\tau}t + \phi]} \tag{5}$$

where ω_0 is the oscillation frequency and $\tau = 2RC = 2Q/\omega_0$ is the energy decay time. The quality factor can be seen as the number of oscillations in a decay time of $\tau/2$.

2.1.2 Transmission line resonator

A transmission line resonator, see Fig. 1b, is characterized by

- its series resistance per unit length $R^\star$ in Ω/m
- its series inductance per unit length $L^\star$ in H/m
- its shunt capacitance per unit length $C^\star$ in F/m
- its shunt conductance per unit length $G^\star$ in S/m

The impedance of an infinitely long lossy transmission line (LTL) is written as

$$Z^{LTL,\infty} = \sqrt{\frac{R^\star + i\omega L^\star}{G^\star + i\omega C^\star}}. \tag{6}$$

In the ideal case of no losses, the impedance reduces to $Z_0 = \sqrt{L^\star/C^\star}$. The propagation constant can be written as

$\gamma = \alpha + i\beta = ((R^\star + i\omega L^\star)(G^\star + i\omega C^\star))^{1/2}$, where α, the real part of γ, also called the attenuation constant, specifies the losses in the transmission line. The phase of the wave is described by β. The input impedance of an open circuited lossy transmission line with length $l = n\lambda/2$, λ being the wavelength of the propagating wave, can be written as

$$Z^{LTL,o} = Z_0 \coth(\alpha l + i\beta l). \tag{7}$$

Around the resonance frequency ω_0 and for small losses α, the input impedance is often approximated as

$$Z^{LTL,o} = \frac{Z_0}{\alpha l + i\pi\frac{\omega-\omega_0}{\omega_0}}. \tag{8}$$

2.1.3 Mapping to LC resonance

Comparing Eq. (3) and Eq. (8), we can map the transmission line resonator to the LCR resonator by simply equating them. The resulting relations are given by the following substitutions

$$R = \frac{Z_0}{\alpha l} \tag{9}$$

$$C = \frac{\pi}{2\omega_0 Z_0} \tag{10}$$

$$L = \frac{2Z_0}{\pi\omega_0} \tag{11}$$

and the quality factor Q can therefore be written as

$$Q = \omega_0 RC = \frac{\pi}{2\alpha l} = \frac{\beta}{2\alpha}. \tag{12}$$

2.2 Coupling Capacitances

In order to interconnect the circuit described above with the input and output lines a capacitive coupling has been used which allows to keep a relatively high Q. The capacitive coupling to the input and the output of the transmission line also enables a transmission measurement, which has been used in our experiments. The modeling of this situation is shown in Fig. 2a with G_{ex} being the real part of the inverse impedance (admittance). On resonance, it is given by

$$G_{ex} = \frac{R_L C_\kappa^2 \omega_n^2}{1 + R_L^2 C_\kappa^2 \omega_n^2} \tag{13}$$

where R_L is the load resistor, C_κ the coupling capacitance and n the n-th harmonic mode of the resonator. An external quality factor can be defined as

$$Q_{ex} = \frac{\omega_n C_n}{G_{ex}}. \tag{14}$$

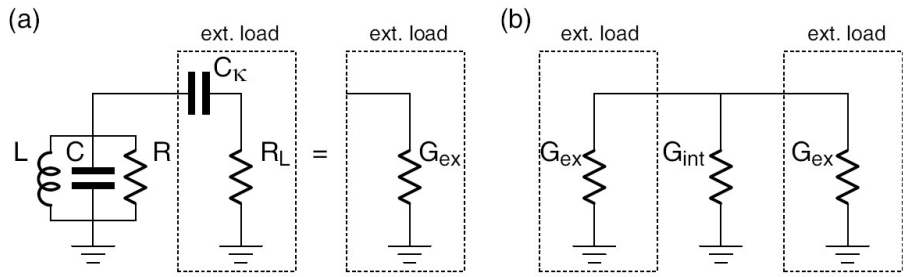

Figure 2: *a) LCR resonator coupled by capacitor C_κ to load a R_l. b) A resonator that is coupled to both, input and output lines. Figure taken from [3].*

where C_n is defined in Eq. (10). For the resonator being symmetrically coupled at the input and output this expression becomes $Q_{ex} = \omega_n C_n / 2G_{ex}$ leading to

$$Q_{ex} = \frac{n\pi}{4Z_0}\left(\frac{1}{C_\kappa^2 R_L \omega_n^2} + R_L\right). \tag{15}$$

The loaded quality factor of the resonator Q_L can be found considering G_{int} and the external shunt conductances G_{ex} being in parallel

$$\frac{1}{Q_L} = \frac{1}{Q_{int}} + \frac{1}{Q_{ex}}, \tag{16}$$

with $Q_{int} = \omega_n C_n / G_{int}$ and the coupling coefficient defined as $g = Q_{int}/Q_{ex}$. An appropriate C_κ can now be chosen in order to obtain the desired Q_{ex} as

$$C_\kappa = \frac{1}{\omega_n} \frac{1}{\sqrt{4Q_{ex} Z_0 R_L/(n\pi) - R_L^2}}. \tag{17}$$

.

2.3 Coplanar Waveguide Resonator

The geometry chosen for the transmission line is a coplanar waveguide (CPW) (for further details on CPW resonators see [2] and [3]). The ground and the center pin lie in the same plane and the ratio of the center pin width to the gap determines the impedance, which should be kept constant. This creates well localized fields in one region of the chip, e.g. where the qubit is positioned, and less intense fields in an other region, e.g. where the dimensions should match with the printed circuit board (PCB). A sketch of a coplanar waveguide with its characteristic parameters is shown in Fig. 3.

The impedance for such a CPW is given by [2]

$$Z_0^{CPW} = \frac{60\pi}{\sqrt{\epsilon_{eff}}} \left(\frac{K(k)}{K(k')} + \frac{K(k_3)}{K(k_3')}\right)^{-1} \tag{18}$$

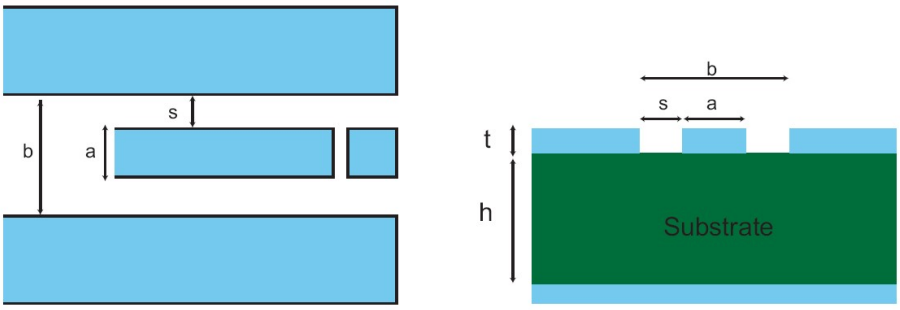

Figure 3: *A conductor backed coplanar waveguide. The ratio s/a determines the impedance Z_0. The length is defined by the position of the gap capacitors. Figure taken from [2].*

with the effective dielectric constant

$$\epsilon_{eff} = \frac{1 + \epsilon_r \widetilde{K}}{1 + \widetilde{K}} \tag{19}$$

where K is the complete elliptic integral of the first kind and

$$\widetilde{K} = \frac{K(k')K(k_3)}{K(k)K(k_3')} \tag{20}$$

$$k = \frac{a}{b} \tag{21}$$

$$k_3 = \frac{\tanh\left(\frac{\pi a}{4h}\right)}{\tanh\left(\frac{\pi b}{4h}\right)} \tag{22}$$

$$k' = \sqrt{1 - k^2} \tag{23}$$

$$k_3' = \sqrt{1 - k_3^2}. \tag{24}$$

ϵ_r is the dielectric constant of the substrate with height h.

The speed of propagation through the CPW is $\nu_{eff} = c/\sqrt{\mu_{eff}\epsilon_{eff}}$, where for non-magnetic substrates $\mu_{eff} = 1$. For a finite length l a resonator has its fundamental resonance frequency at

$$\omega_0^{CPW} = \frac{\pi}{l}\frac{c}{\sqrt{\epsilon_{eff}}}. \tag{25}$$

3 Fabrication

In order to be able to understand how to fabricate and reproduce resonators with high quality factors, it is important to diversify substrates of resonators. Diversifying substrates also helps to explain losses in more details. I have been working with four different substrates.

- Si wafer, provided by Yale, of thickness $t_{\mathrm{Si}} = 275\,\mathrm{um}$, followed by a wet oxidized Silicon SiO_x layer of thickness $t_{\mathrm{SiOx}} = 550\,\mathrm{nm}$ and a Nb film of thickness $t_{\mathrm{Nb}} = 190\,\mathrm{um}$.
- Si wafer, provided by Karlsruhe, of thickness $t_{\mathrm{Si}} = 500\,\mathrm{um}$, followed by an oxidized Silicon SiO_x layer of thickness $t_{\mathrm{SiOx}} = 290\,\mathrm{nm}$ and a Nb film of thickness $t_{Nb} = 150\,\mathrm{nm}$.
- Si wafer, provided by Yale, of thickness $t_{\mathrm{Si}} = 500\,\mathrm{um}$, followed by a thermally oxidized Si layer of thickness $t_{\mathrm{SiOx}} = 550\,\mathrm{nm}$ and an Al film of thickness $t_{\mathrm{Al}} = 200\,\mathrm{nm}$
- Si wafer, provided by Karlsruhe, of thickness $t_{\mathrm{Si}} = 500\,\mathrm{um}$,with no oxide, followed by a Nb film of thickness $t_{\mathrm{Nb}} = 150\,\mathrm{um}$.

Sapphire appears to be an excellent candidate to be used as a substrate, since it would avoid the uncertainties one have with the oxidation of silicon and it should have lower losses at these temperatures and frequencies. Two inch diameter wafers with either Nb or Al as superconducting materials have been used. Their respective superconducting transition temperatures are 9.2 °K and 1.2 °K. Consequently for the Nb resonators, measurements in liquid helium(4.2 °K) are possible.

The fabrication process is done in the ETH clean room facility FIRST.

Spinning on resist

The process starts with cleaning the wafer

- 10 min bath in acetone
- 5 min bath in isopropanol that eliminates the remaining acetone on the wafer
- 5 min in water.
- Drying for 5 min at 200 °C on a hot plate.

A 500 nm thick photo resist layer is added to the wafer. The wafer is put on the spinner for 60 sec at 3000 rpm. The cleanliness of the wafer cannot be over-emphasized, so that it is recommended between every step to clean it briefly with acetone, isopropanol.

Photolithography-Development

Exposing the photo resist (characterized by its exposure time) through a mask for 82 sec under a 4.3 mWcm^{-2} optical lithography lamp (MA6 mask aligner) gives rise to the resonators pattern. We used the same mask for all

our wafers. The light breaks the polymer structure of the resist, leaving the shaded part of the resist intact. The wafer is placed in a bath of developer for 1 min 20 s. The developer gets rid of the broken resist structures and the Nb layer appears on the surface. Again, wafer is cleaned.

Ion etching

In the next step of the fabrication process, the wafer undergoes reactive ion etching (RIE). This will eliminate the Nb layer that lies on the surface. An Argon-SF6 recipe is used and the etching time carefully determined. All Niobium has to be gone because traces of this material would cause the resonator to be shorted. It is also very important not to etch to long into the silicon oxide. This layer should be affected the least possible in order to avoid conductivity problems and enhanced dielectric loss.

	Si	SiO_x	resist	Nb	PMMA
etch rate [nm/min]	186 ± 5	31 ± 4	$56 \pm 1/83 \pm 7$	85 ± 3	121 ± 2

Table 1: Etch rates taken from [4]

Dicing and Mounting

After etching, the wafer is cleaned for an hour in an acetone bath and then spanned on a blue tape. The dicing will give us the 3x8 mm chips. Chips are cleaned in a 15 min ultrasonic acetone bath at 50 °C, and then left there for an hour. After rinsing the chips with isopropanol, they are ready to be mounted and bonded.

The chips are mounted on a PCB circuit board, which was cleaned before in citric acid and isopropanol. We used the resist PMMA to glue the chips.

Bonding

At the end of the fabrication process, chips are bonded. A simplified procedure for making an ultrasonic wire bond is shown in Fig. 5.

1. Wire is placed between the bonding surface of the tool and the bond.
2. The tool is lowered to the edge of the resonator chip and presses the wire against the surface with a predetermined force. Ultrasonic energy is used to make the bond.
3. The tool is raised slowly and pulls the wire from the spool.
4. The tool is positioned to the edge of the copper surface of the PCB while forming a loop.

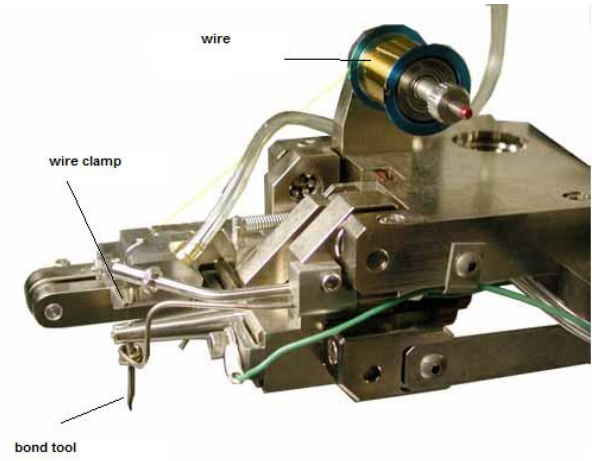

Figure 4: Wire bonder

5. The second bond is made as described in 2.

6. At the end, a wire clamp, placed behind the tool, closes and pulls back on the wire to break it. The tool is raised again, and the bonder is ready for the next cycle.

The bonds are kept rather short in order to avoid excess impedances at microwave frequencies due to the inductance of the bond wire. As many bonds as possible on the inner conductor are recommended. Depending on the resonator's superconducting material, Al or Nb, different parameters for the bonder are used. Tab. 2 shows the parameters used for Nb resonators.

Time(Bond 1/Bond 2)	30/30ms
Power(Bond 1/Bond 2)	280/400
Force(Bond1 /Bond 2)	Low/High
Wire pull	29
Wire tail	60
Height	10
Wire	Hard Aluminum

Table 2: Bond parameters for Nb

The fabrication process is done and the chips are ready to be characterized. A picture of a bonded resonator chip, mounted on a printed circuit board (PCB), is shown in Fig. 6

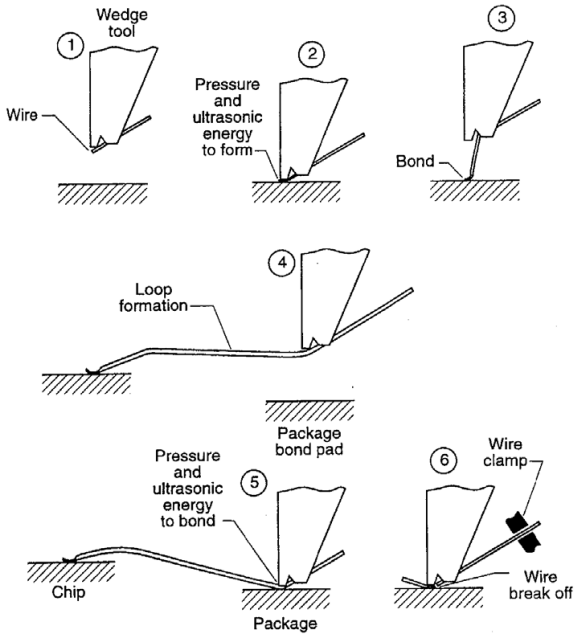

Figure 5: Simplified procedure for making a wire bond

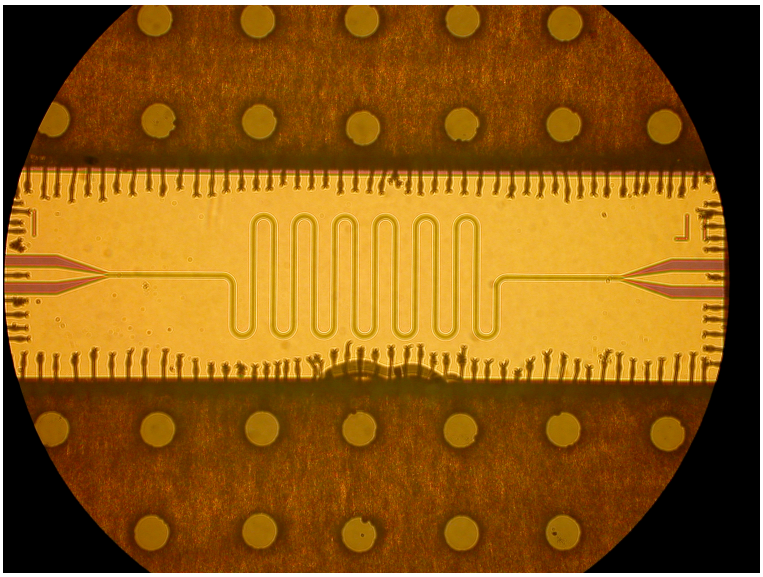

Figure 6: Resonator chip after bonding

4 Experiment

A coplanar waveguide resonator has three main parameters:

1. the resonance frequency ν_r mainly determined by its length and the propagation constant, but also slightly affected by the coupling capacitance.

2. the external quality factor determined by the capacitors

3. the impedance determined by the ratio of the center conductor width to the size of the gap between the center conductor and the ground planes (set to 50 Ω).

As long as it does not affect the transmission, the resonance frequency can be set arbitrarily by just adapting the length. In absence of coupling capacitors, the frequency is given by Eq. (25), otherwise it is slightly shifted, as mentioned above. ϵ_{eff} is the effective dielectric constant of the substrate.

The external quality factor depends on the design of the coupling capacitances. For the undercoupled case, i.e. large external quality factors, the capacitor is simply a gap, see Fig. 8. For the overcoupled case, the capacitances can be made arbitrarily larger by adding more and more fingers. The limit is set by the optical lithography process. The relation between capacitors and external quality factors is given by Eq. 15.

In the undercoupled case, we will measure the internal quality factor, while in the overcoupled case we will measure the external quality factor. Measuring these parameters along with the resonance frequency and comparing them to simulations and theory is the main goal of this work.

4.1 Experimental setup

For the sample mount we want to avoid electromagnetic stray fields as well as unwanted reflections due to impedance mismatches in the connections of the circuit. The sample mount was made out of solid copper and right angle surface mount SMP connectors with good performance up to about 20 GHz that were used to direct the signals to the printed circuit board. Finally bullet connectors were used to connect coaxial lines to the sample mount. A sample holder similar to the one shown in Fig. 7 was used.

The sample holder is connected to coaxial lines that are confined within a 1.5 m long dipstick which is slowly immersed in a tun filled with liquid Helium at 4.2 K. The cool-down process of the dipstick takes about ten minutes. When the superconducting regime is reached, the dipstick is connected to a Vector Network Analyzer (VNA) through coaxial cables. DC blocks are used at the in- and output of the VNA and the input power of the VNA was chosen to be in general between -20 dBm and -50 dBm. After choosing the right settings (input power, averaging, span, sweep time, attenuation and calibration), transmission curves can be recorded.

The resonator frequency response measured in transmission exhibits a Lorentzian line shape, as expected for a driven harmonic oscillator. Its trans-

Figure 7: *Sample mount made from copper and one cent coin for size scale. Also shown is the chip containing the sample, the PCB and necessary connections.*

mission power spectrum is given by

$$P(\nu) = P_0 \, \frac{\delta\nu_0^2}{(\nu - \nu_0)^2 + \delta\nu_0^2}, \tag{26}$$

(taken from [3]), where $\delta\nu_0$ is the half width at half maximum of the Lorentzian line, ν_0 the bare resonance frequency and P_0 the maximally transmitted power at a given input power.

4.2 Data

From our transition measurements, we can determine directly the following parameters:

- the resonance frequency, given by the position of the peak,
- the loaded quality factor, given by the half width at half maximum,
- the insertion loss, given by the magnitude of the peak.

Eq. (25) relates the resonance frequency to the length of the resonator and to the dielectric constant of the substrate. The latter one will be dependent of the substrate.

The loaded quality factor can be written by means of the internal and external Q as seen in Eq. (16). In the overcoupled case, i.e. large coupling capacitances, i.e small external Qs, the measured quality factor will be equal to the external Q. In the undercoupled case, i.e. small coupling capacitances, the measurement will give us the internal quality factor.

We used the same mask on all the wafers. Each resonator is labeled by a letter and a number. The letter indicates the type of coupling capacitances the resonator have (finger, fingers, gaps) whereas the number indicates to which serie it belongs, i.e. its resonance frequency. The series is characterized

by the length of the resonator, and therefore useful for resonance frequency approximations. In particular, we measured the resonators labeled K, J and L, M, as shown on Fig. 8. There were three series of these K, J, L, M resonators. Series 1,2,3 have their resonance frequency respectively around 3.5 GHz, 5.8 GHz and 8.2 GHz. The design for the resonators K, J, L, M was the following.

- finger coupling capacitances: L1, L2, L3 and M1, M2, M3. The fingers were 97 um long, where L has one finger and M four. Resonators with these capacitances are overcoupled, e.g. the measured Q should be the external Q, and the insertion loss 0 dBm.
- gap capacitances: J1, J2, J3 and K1, K2, K3. The gap dimensions are 10x10 um for J and 10x30 um for K. The measurement gives us the internal Q of the resonator, which we can assume to be the same for all resonators from one series.

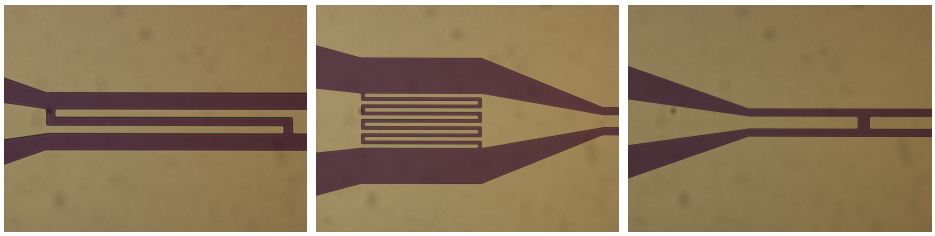

Figure 8: *Left picture: L resonator-one finger capacitance with length of 97 um. Middle: M resonator-four finger capacitance with length of 97 um. Right: J resonator-gap capacitance with dimension* $10x10$ *um*

5 Characterization

5.1 Simulation

As we have seen before, the mapped LCR model works great for frequencies close to the resonance frequency. From Eqs. (9 - 11), we can find the following relation:

$$\omega_0 = \frac{1}{\sqrt{(C + C_k)L}} \tag{27}$$

where C_k is the coupling capacitance. In case of gap capacitors, e.g. small capacitances values, as for J and K, the resonance frequency will hardly be affected. In case of finger capacitors, the resonance frequency will be shifted by

$$\Delta\omega = -\frac{\pi C_k}{2C(C + C_k)Z_0} \tag{28}$$

The shift of the frequency is due to the loading governed by the capacitor and is negligible for gap capacitances, but very pronounced for finger capacitances as seen in the previous section. It adds an additional, effective, so-called electronic length to the resonator which is not given just by the finger length. The mapped LCR model fails for off-resonance regions. Another model that overcomes this problem is the scattering matrix model for CPW and it is extensively discussed in [1]. The model calculates the transmission spectrum, and is supposed to fit the experimental curve. The matrix is given by

$$\begin{pmatrix} A & B \\ C & D \end{pmatrix} = \begin{pmatrix} 1 & Z_{in} \\ 0 & 1 \end{pmatrix} \begin{pmatrix} cosh(\alpha + i\beta l) & Z_0 sinh(\alpha + i\beta l) \\ Y_0 sinh(\alpha + i\beta l) & cosh(\alpha + i\beta l) \end{pmatrix} \begin{pmatrix} 1 & Z_{out} \\ 0 & 1 \end{pmatrix} \tag{29}$$

and

$$Z_{in/out} = \frac{1}{2\pi i f C_{in/out}} \tag{30}$$

where $Z_{in/out}$ are the in- and output impedances, closely related to the in- and output coupling capacitors. α can be determined from the measured quality factor and insertion loss, therefore from experimental data, and β can be expressed as a function of the dielectric constant. The transmission line spectrum is then

$$S_{21} = \frac{2}{A + B/Z_{L0} + CZ_{L0} + D}. \tag{31}$$

The task is to adapt the unknown variables in order to match the experimental plots. These variables are:

- effective dielectric constant
- coupling capacitances

- effective electronic length

The measurement of transmission curves for the resonators K1-3, J1-3, M1-3, L1-3 is done under the same environmental conditions (temperature, calibration and input power).

5.2 Comparison

In the previous section, we have seen how to obtain some properties of a CPW resonator from experimental data such as resonance frequency, insertion loss, etc ... The internal Q factor for example was found for resonators, belonging to the same series, by taking the value of the measured quality factor of the resonator with the smallest capacitance (in this case, a gap capacitance, more likely the K resonator). The length of the resonator with gap capacitances can be easily measured on the mask. The gap capacitances itself can be determined by finite element simulations. Problems however arise when it comes to determine the dielectric constant of materials such as silicon or silicon oxide or the length of resonator with finger capacitances or their values. The goal is to find a standard procedure that completely characterizes resonators. We will only show results for the wafer, provided by Yale with silicon oxide and aluminum.

1. The first step in the characterization is to determine the effective dielectric constant. We start with the resonator with the smallest capacitance, i.e. K1, K2, K3. The capacitance is a gap dimensions of 10×30 um. We know its length through measurements on the mask, and the capacity has been determined by simulations. Therefore, the only variable that changes the shape of the transmission spectrum in Eq. (31) is ϵ_{eff}. In Fig. 9, the experimental and theoretical plots match and $\epsilon_{eff} = 5.066$ for this substrate. We used resonator J1 which is a gap capacitor with dimensions of 10×10 um and is shown in Fig. 8. We compared the measured transmission spectra of an Al resonator on Si oxide substrate at $T = 20\,\mathrm{mK}$ to theory. The capacitor value and length are determined respectively by simulation and measurements. The effective dielectric constant ϵ_{eff} has been adjusted such that the theoretical curve fits the experimental plot and was found to be $\epsilon_{eff} = 5.066$ with coupling capacitance $C_k = 0.4$ fF and length $l = 8990$ um.

2. Having determined the effective dielectric constant, we assume that its value is the same for every resonator on the wafer. There are now only two 'fit' parameters left, the length of the finger capacitors and their values. Changing the length of the resonator affects only the position of the resonance frequency, so that we only have to fit the capacitances in order to adjust the shape of the theoretical curve to the experimental

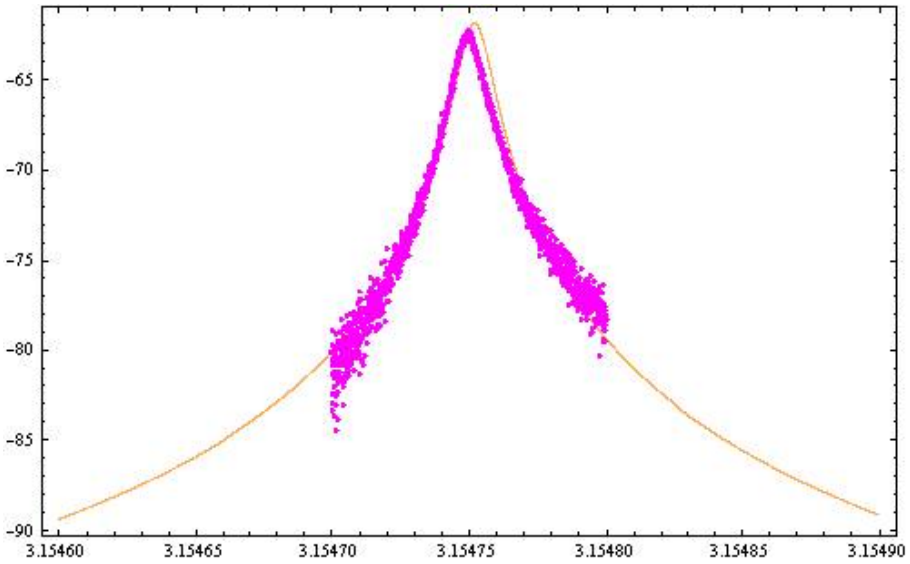

Figure 9: Measured transmission spectra of Al resonators on Si oxide substrate with 10 um gap capacitors in comparison to theory(solid lines) at base temperature 20mK. $\epsilon_{eff} = 5.066$ determined from fitting J1 resonator with coupling capacitance $C_k = 0.4$ fF and length $l = 8990$ um.

one. Capacitances of M1 and L1 are found. Capacitances of M2, M3 and L2, L3 have respectively the same geometrical shape as M1 and L1 and therefore the same values as M1 and L1.

3. Knowing all the capacitances, we are now in a position to determine the effective electronic length of resonators with finger capacitances (L and M). The remaining 'fit' parameter is now the length and the results for Al resonators on Si oxide are shown in Fig. 10 . We measured Al L-resonators from series 1-3 on Si oxide with one finger capacitors (length of 97 um, also shown in Fig. 8) at $T = 20$ mK. The fit parameter is the length difference that must be subtracted from the length of the finger: $\Delta l = l' - l$ where l' is the effective electronic length and l is the length of the resonator taken from the beginning of the input coupling capacitance to the end of the output capacitance. Δl counts the length to subtract for both fingers at the in- and output and is consistently 60 percent of the finger length. The finger capacitance therefore adds an electronic length to the resonator of approximately 40 percent of its length on both in- and output coupling capacitances. This is consistent for all finger capacitances, independent of the number of fingers.

4. Applying all previous results, the theoretical curve matches the experimental results, as shown on Fig. 11. This procedure can be applied

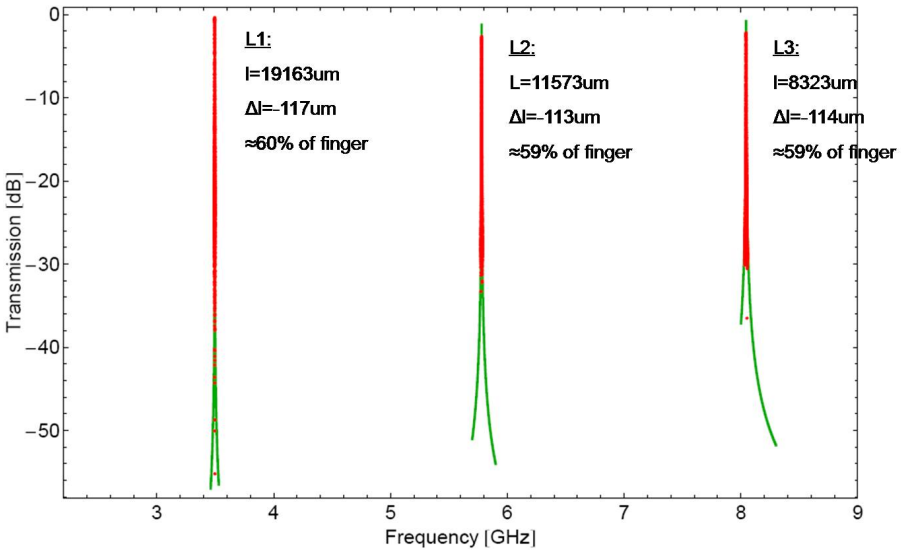

Figure 10: Al L-resonators from series 1-3 on Si oxide with one finger capacitors (length of 97um) at base temperature.

to further resonators on the mask, and a complete characterization of the wafer is possible.

The consistency can be checked by considering the high Q resonators from series 1 to 3. The internal Q factor and the coupling capacitances are set constant throughout the series, using ϵ_{eff} as a fit parameter. The results are shown in Fig. 12. Small differences in the value of the dielectric constant throughout the wafer can be explained by the uncertainties of the oxidation process of silicon. As for other materials like pure silicon, fabrication process can affect the substrate irregularly. The results found for the resonators of series one can be applied to the resonators of series two and three. Using the same values for dielectric constant, coupling capacitances and subtracting 60 percent of the finger's length to the total length, we can see on Fig. 13 that the theoretical curves match the experimental plots. This procedure can be extended to more resonators on the wafer as well as to wafers with different substrates. Results of measurements of these resonators can therefore be understood within scattering matrix models and also using mapping to a simple parallel LCR.

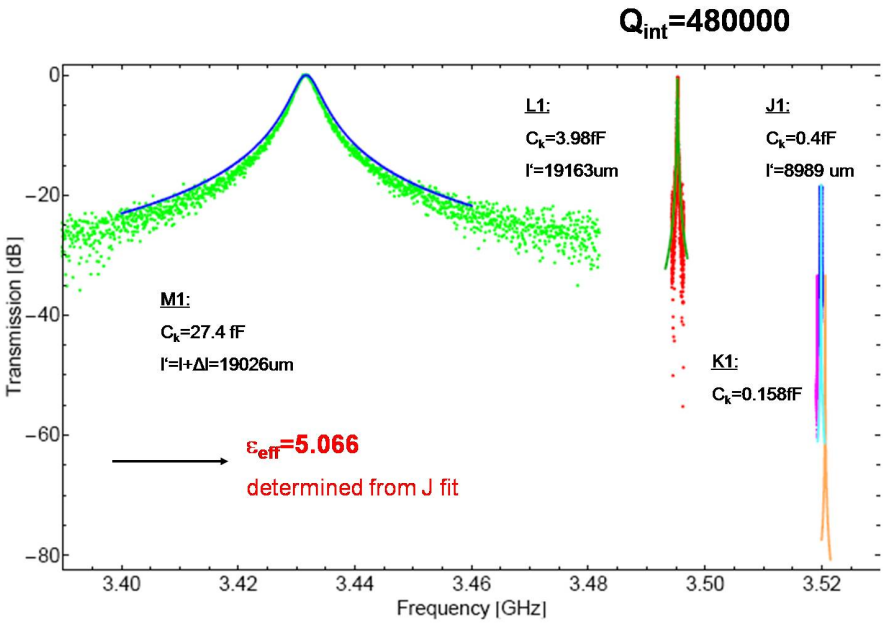

Figure 11: Plots of all four resonators K,J, L and M from series 1, from wafer Al on Si oxide, and measured at $T = 20$ mK. Values of capacitances, effective length and the dielectric constant are displayed next to the curves. It is a successful test for the mapped LCR and scattering matrix model

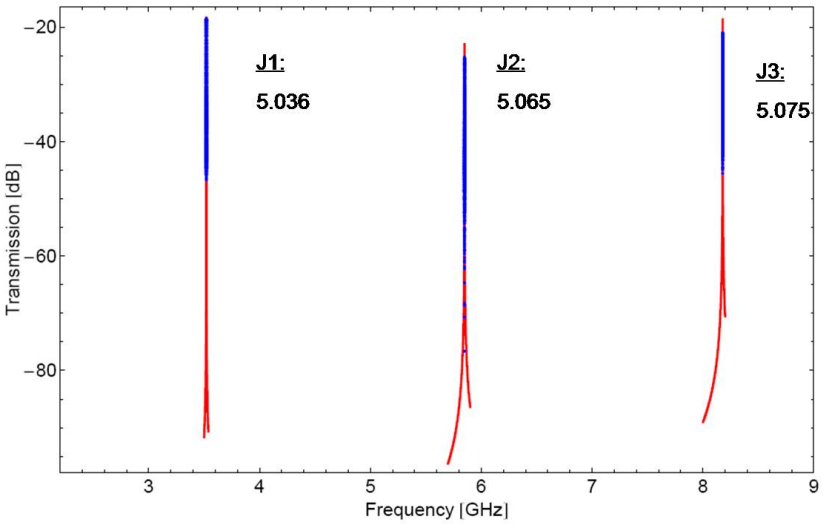

Figure 12: Comparison of J1, J2, and J3 resonators and their corresponding effective dielectric constants. Lengths and capacitances are kept constant for each series. One can see small variations, best explainable by uncertainties in the oxidation parameters of silicon

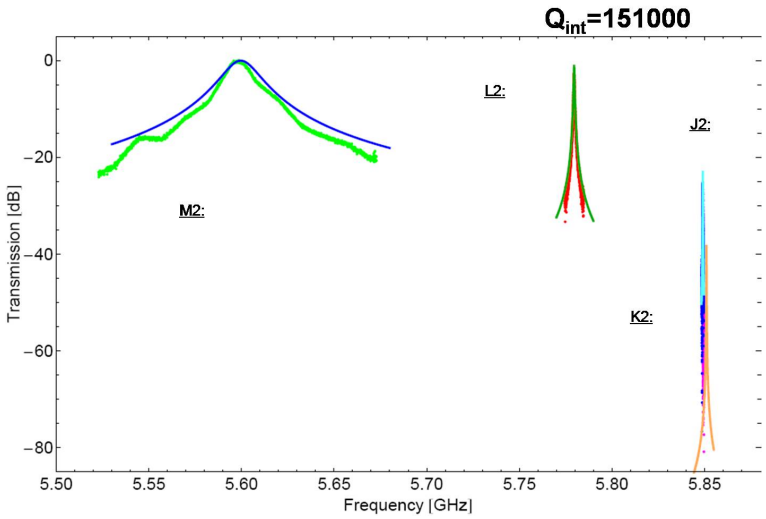

Figure 13: Resonators M2, L2, K2 and J2 of Al on silicon oxide wafer, and measured at $T = 20$ mK. Same capacitances and effective dielectric constant as in Fig. 11 are used. 60 percent of the finger's length is subtracted from the total length.

6 Conclusion

The CPW resonator acts as a cavity. In order to proceed to the fabrication of the qubit, as good as possible knowledge of the properties of the resonator is required, i.e. internal Q-factor, resonance frequency, insertion loss... In this semester work, we worked out a standard procedure to characterize the properties of the wafer, such as the dielectric constant, the coupling capacitances and the effective length. The main results are

- We are able to design and realize resonators with parameters required for Circuit QED and measurements are explained by scattering matrix model and using mapping to a parallel LCR circuit very successfully.
- The effective length of finger capacitance $l' = l - 2\Delta L$ with $\Delta L \approx 3/5 l_{\text{finger}}$ and l being the length of the resonator measured from the beginning of the input coupling capacitance to the end of the output coupling capacitance.
- Coupling capacitances shift the resonance frequency
- Variations in effective dielectric constants throughout the wafer are explained by local variations of the substrate and uncertainties in ϵ_{SiOx}.

Acknowledgment

I would like to thank Prof. A. Wallraff for giving me the opportunity to participate in an interesting and exciting project of his research group. I am thankful to P. Leek, M. Goeppl and A. Fragner for their valuable guidance and to the rest of the group for its great and friendly ambiance.

References

[1] D.M. Pozar: *Microwave Engineering*, Addison-Wesley Publishing Company, 1993

[2] J. Fink: *Single Qubit Control and Observation of Berry's Phase in a Superconducting Quantum Circuit*, Diploma Thesis, ETH 2007

[3] A. Wallraff, H. Majer, L. Frunzio, and R. Schoelkopf: *Superconducting solid state cavity QED: Notes on resonators*, 2003

[4] P. Studer: *High Q resonators for Quantum Information Processing*, Semester thesis, ETH 2007